San Jose State University
SJSU ScholarWorks

Faculty Publications, Chemistry | Chemistry

11-1-2011

Chemical activity in YBa2Cu3O7 – δ across the normal to superconducting phase transition

Juana Vivó Acrivos
San Jose State University, juana.acrivos@sjsu.edu

Follow this and additional works at: http://scholarworks.sjsu.edu/chem_pub

 Part of the Physical Chemistry Commons

Recommended Citation
Juana Vivó Acrivos. "Chemical activity in YBa2Cu3O7 – δ across the normal to superconducting phase transition" *Microchemical Journal* (2011): 239-245. doi:10.1063/1.1701808

This Article is brought to you for free and open access by the Chemistry at SJSU ScholarWorks. It has been accepted for inclusion in Faculty Publications, Chemistry by an authorized administrator of SJSU ScholarWorks. For more information, please contact scholarworks@sjsu.edu.

Chemical activity in $YBa_2Cu_3O_{7-\delta}$ across the normal to superconducting phase transition

JV Acrivos,

San José State University, San José CA 95192-0101

Abstract

The Gibbs free enthalpy, chemical activity across the transition temperature to superconductivity, T_c in $YBa_2Cu_3O_{7-\delta}$ is obtained from reciprocally enhanced X-Ray absorbance, XAS and diffraction, XRD data near the Ba $L_{3,2}$ edges' energy E_a, and orientations in the X-ray beam for preferred Miller indexed [HKL] planes' scattering that are enhanced near T_c. The standard enthalpy and entropy for the formation of mixed normal metal/superconducting domains above T_c, determined individually across the two Ba $L_{3,2}$ edges, to better than a percent accuracy: $\Delta H^{\neq}_{\geq}$=-220 meV, and $\Delta S^{\neq}_{\geq}$=-2 meV/K when $121 \geq T \geq 92K \approx T_{c1}$, indicate there is energy available to form the mixture and the reduced entropy indicates there is also order increase. Below T_c the standard enthalpy and entropy to form at least two mixed superconducting phases is halved to $\Delta H^{\neq}_{\leq}$ = -86 meV, $\Delta S^{\neq}_{\leq}$= -1 meV/K when $92K \geq T \geq T_{c2} \approx 72K$. Thus reciprocal XAS/XRD enhancement at orientations in the X-ray field, of preferred 2D planes, induced by the transition to superconductivity in the layer solid, indicates one, the importance of the 2D-plane electron density scattering near T_c, and two, identifies the 2D-plane chemical activity, by the electron density leading to symmetry allowed excitations, a role similar to that of the electron density in linear bonds for molecular activity.

Introduction

This work uses the Onsager reciprocity relation expected for enhanced X-ray absorption spectroscopy, XAS and co-incident diffraction, XRD at preferred orientations versus temperature, T near the phase transition to superconductivity, T_c including all the layers of $YBa_2Cu_3O_{7-\delta}$, to enrich the literature on layer materials[1,2]. Pauling describes the role played, in the phase transition by resonance between two Cu=O at 90° angles in the CuO_2 layer[1*l*] which is included in most models that explain the importance of the CuO_2 layer. But, to understand the periodic lattice distortion, PLD effects proposed by Overhausser[2c] and the de Gennes boundary effect arguments[2d] the role played near T_c by other than the CuO and CuO_2 layers is necessary. In $YBa_2Cu_3O_{7-\delta}$ and $Bi_2Sr_2Ca_2O_3O_{10+\delta}$, the appearance of superconductive domains has been deduced by the presence of Abrikosov vortices at ~60 K above T_c[2h,p], when it is determined by bulk measurements of heat capacity and susceptibility[1g,2k-o]. At temperatures where the thermal fluctuation energy is comparable with the elastic and the pinning energy of vortices other stabilizing interaction must be present. This work obtains the chemical activity, measured by the standard Gibbs free enthalpy for the formation[2w] of normal/superconducting mixed states using reciprocally enhanced XAS and preferred XRD reflections data[1a-i] versus temperature to identify how the different layers in $YBa_2Cu_3O_{7-\delta}$ are involved across T_c.

Experimental

The published enhanced absorbance and diffraction data used was obtained by XAS and XRD synchrotron measurements at DOE National Laboratories SLAC-SSRL, LBL-ALS[1a-e]. I(hν)=(detector counts)/(monitor counts) versus near energy, E_a (fig. 1-4) for different $YBa_2Cu_3O_{7-\delta}$ samples are used: a single crystal grown by CT Lin[1k] and $NdBa_{1.9}Nd_{0.1}Cu_3O_{7-\delta}$ powder grown by KK Singh at IRC for Superconductivity, Cavendish Laboratory[1b], and 30nm $YBa_2Cu_3O_{7-\delta}$ films on [001] $SrTiO_3$, grown by MA Navacerrada at the Complutense University[1e]. Calibration with CuO standards allow E_a comparison versus T to better than ±¼eV. Incident and transmitted X-Rays near a constituent resonance energy, E_a along $\mathbf{k}_0$, are scattered along $\mathbf{k}_s$ with the polarized electric field $\boldsymbol{\varepsilon_0}$, $\boldsymbol{\varepsilon_s}$ in the plane of incidence, and scattering $Q=|\mathbf{k}_s-\mathbf{k}_0|=4\pi\, n(E_a)\, E_a \sin\theta_{Bragg}/hc \approx G_{[HKL]}=2\pi((H/a)^2+(K/b)^2+(L/c)^2)^{½}$, leads to Stenström shifts due to index of refraction $n(E_a)$, $\Delta E_a=E_a(n(E_a)-1)/\sin^2\theta$ [1j], and its critical oscillations[2q] near phase transitions (fig. 4b). Orientation in the X-ray beam cryostat is given by $\beta_{[001]}=\mathbf{k_0}\wedge\mathbf{c}_{axis}$, and

the field projection $\phi_{[001]}=\boldsymbol{\varepsilon}_{[001]}\hat{}\mathbf{a}_{axis}$, and [HKL] reflections occur when the Bragg condition, $\sin\theta_{Bragg}=2\pi L/c/Q\cos\beta_{[001]}-(1-(2\pi L/c/Q)^2)^{1/2}\sin\beta_{[001]}\cos(\phi_{[001]}-\phi_{[HKL]})$, is satisfied (Table **I**).

Discussion

The strong Ba $L_{3,2}$-E_a enhanced absorbance data across T_c (fig. 2) is used to identify the chemical activity near the BaO layer, which is consistent with the other elements' edge enhancement[1a-d] (fig. 1, 3, 4). The growth and chemical activity in a solid is determined by the 2D reactive Q=[HKL] reflection planes' electron density, in the highest occupied and lowest unoccupied extended states E_HOMO and E_LUMO, which also determine the transition temperature to superconductivity, in a manner similar to the role of reactive linear bonds in molecular activity. Accurate data for transitions from the constituent elements core states to the lowest unoccupied extended states, E_LUMO near the Fermi energy, in $YBa_2Cu_3O_{7-\delta}$, measured versus T in cycles from room temperature (RT) to liquid He (4K) and back[1b-e] (fig. 1-4):

$$\mathcal{Q}:|i(\text{core atomic state})> \Rightarrow |f(\text{E\_LUMO})>, \tag{1}$$

e.g.,

$$|i,O(1s)^2.> \Leftrightarrow |f(\text{E\_LUMO},O:(1s)^{\cdot\cdot}np)>,$$

$$|i,Y(1s)^2.> \Leftrightarrow |f(\text{E\_LUMO, O:}(1s)^{\cdot\cdot}np)>,$$

$$|i,Cu..(2p_{3/2})^4(2p_{1/2})^2\,(3d)^{10}to(3d)^9> \Leftrightarrow |f(\text{E\_LUMO, Cu:.}(2p_{3/2})^3(2p_{1/2})^2\,(3d)^{10}\text{ to }(3d)^9\,nd_{5/2})>$$

$$|i,Cu..\,(2p_{3/2})^4(2p_{1/2})^2\,(3d)^{10}to(3d)^9> \Leftrightarrow |f(\text{E\_LUMO, Cu:.}(2p_{3/2})^4(2p_{1/2})\,(3d)^{10}\text{ to }(3d)^9\,nd_{3/2})>,,$$

$$|i,Ba..\,(2p_{3/2})^4(2p_{1/2})^2.> \Leftrightarrow |f(\text{E\_LUMO, Ba:.}(2p_{3/2})^3(2p_{1/2})^2\,.(nd_{5/2})>,$$

$$|\,i,Ba..\,(2p_{3/2})^4(2p_{1/2})^2.> \Leftrightarrow |f(\text{E\_LUMO, Ba:.}(2p_{3/2})^4(2p_{1/2})\,.(nd_{3/2})>.$$

describe the transition probability by the induced moment squared:

$$|\mathbf{M}_{\mathbf{Q}a}|^2 = |<i|\exp(-i\mathbf{k}_0\cdot\mathbf{R}_a)\boldsymbol{\varepsilon}_0\cdot\delta\mathbf{R}_a|f><f|\exp(i\mathbf{k}_s\cdot\mathbf{R}_a)\boldsymbol{\varepsilon}_s\cdot\delta\mathbf{R}_a|i>|, \tag{1.1}$$

when $\boldsymbol{\varepsilon}_0$, $\boldsymbol{\varepsilon}_s$ have non-zero components in the reflection plane Q at the Bragg condition. $\delta\mathbf{R}_a$ is the charge displacement at atom $\mathcal{Q}$ by the polarized synchrotron radiation, and the final states obey the symmetry selection rules. The extended states, may be described in a first order approximation by the superposition of individual layer wave functions, Ψ_{layer} obtained by self consistent field molecular orbital calculations, weighted by a factor, $\alpha_{\mathbf{Q},layer}$ in a tight binding approximation[1f,h]:

$$|\mathbf{Q}\rangle=\Sigma_N\Sigma_l\{\alpha_{\mathbf{Q},CuO_2}\Psi_{CuO_2,l}+\alpha_{\mathbf{Q},BiO}\Psi_{BiO,l}+\alpha_{\mathbf{Q},SrO}\Psi_{SrO,l}+\alpha_{\mathbf{Q},Ca}\Psi_{Ca,l}\}/\sqrt{N}. \quad (1.2)$$

At energies far from resonance absorption, and at temperatures far from a phase transition, XRD is analyzed using the kinematical approximation for $I(\mathbf{Q})=I_s/I_0$ to obtain the scattering power[2a]:

$$S_{\mathbf{Q}} = \int_{\mathbf{Q}\pm2(WHH)} I(\mathbf{Q}')\, d\mathbf{Q}'/\int_{\mathbf{Q}\pm2(WHH)} d\mathbf{Q}' = |\mathbf{F}_{\mathbf{Q}}|^2 A_m(E,\mathbf{Q}) \quad (2)$$

where the total material absorption, A_m depends on the radiation path, $d/\sin\theta$ and its tabulated linear absorption coefficient[2g]; d=6.4±1 μm, for CT single crystal thickness where uncertainty, especially at the Y K-edge is introduced by strong XRD enhancement and index of refraction oscillations (fig.4b). In three dimensional solids, both the scattering power and chemical activity at a site **R** depend on the lattice potential:

$$V(\mathbf{R}) = \Sigma_{[HKL]} V_{\mathbf{Q}=[HKL]} e^{i\mathbf{Q}\bullet\mathbf{R}}, \quad (2.1)$$

where the Fourier component, $V_{[HKL]}$ is proportional to[2a]:

$$F_{\mathbf{Q}} = \Sigma_{\text{lattice sites } l} f_{Q,l}\, \alpha_{\mathbf{Q},l} \quad (2.2)$$

Contributions from constituent element electron density scattering power, f_{Ql} (f^0_{Ql} are tabulated at energies far from a resonance absorption[2g]) and $\alpha_{\mathbf{Q},l} = \exp(i\mathbf{R}_l\bullet\mathbf{Q}+\phi_i)$). In layer materials the occupied sites $\mathbf{R}_l$ are usually displaced from the ideal Space Group site $\mathbf{R}_l^0$, by $\boldsymbol{\delta}_l = \sum_q \mathbf{u}_q \exp(i(\mathbf{R}_l\bullet\mathbf{q}+\phi_q)$, due to periodic lattice distortions, PLD chemical waves, $\mathbf{q}=(q_x,q_y,q_z)$, then:

$$\alpha_{\mathbf{Q}+\mathbf{q},l} = \sum_{\text{unit cell equivalent } l} \exp(i(\mathbf{R}_l+\boldsymbol{\delta}_l)\bullet\mathbf{Q}),$$

simplified by the Jacobi-Anger theorem[2c,e]:

$$\alpha_{\mathbf{Q}+\mathbf{q},l} = \sum_l \sum_{\mathbf{q},n=0,\pm1,..} J_n(z_{q,\mathbf{Q}}) \exp(i(\mathbf{Q}+n\mathbf{q})\bullet\mathbf{R}_l+\phi_q),$$

identifies the Bragg reflections at $\sum_{l,\mathbf{q}}(\mathbf{Q}+n\mathbf{q})\bullet\mathbf{R}_l+\phi_q = 2\pi m$, (m, n = integers), when n PLD sidebands about a center band, are separated by $\mathbf{q}\bullet\mathbf{Q}/|\mathbf{Q}|$, the $J_n(z_{\mathbf{q},\mathbf{Q}})$ are 1st order Bessel functions with **Q** dependent argument $z_{\mathbf{q},\mathbf{Q}}=\mathbf{u}_q\bullet\mathbf{Q}$, evaluated from the relative sideband to center band intensity, $I_n/I_0=|J_n(z_{\mathbf{q},\mathbf{Q}})/J_0(z_{\mathbf{q},\mathbf{Q}}))|^2$ and there may be more than one $|\mathbf{q}|<<|\mathbf{Q}|$. The PLD waves in $YBa_2Cu_3O_{7-\delta}$, $q_{xy}=2\pi/12(a^2+b^2)^{1/2}$ determine the reflection plane Q scattering power[1e] and the chemical activity by interference between transmitted, T_j and reflected the S_j waves, at the j^{th}

layer (fig. 1). Near an absorption energy, E_a resonant scattering terms and neighbor, l dependent extended X-Ray absorption fine structure, XAFS χ in condensed matter respectively obtain[2a,b]:

$$F_{\mathbf{Q},a} = A_{0,\mathbf{Q}} + \sum_l C_{l,\mathbf{Q}}, \qquad (2.3)$$

where,

$$A_{0,\mathbf{Q}} = F^0_{\mathbf{Q}} + \alpha_{\mathbf{Q}a}\,(f'+i\,f'')_{\mathbf{Q}a}, \qquad F^0_{\mathbf{Q}} = \sum_l \alpha_{\mathbf{Q}l}\, f^0_{\mathbf{Q}l}, \qquad C_{l,\mathbf{Q}} = f''_a\,\alpha_{\mathbf{Q}a}\,(\chi'_{al} + i\,\chi''_{al}),$$

$$(f'+i\,f'')_{\mathbf{Q}a} = |\mathbf{M}_{\mathbf{Q}a}|^2\, r_0\,(\Delta_a + \tfrac{1}{2}\,i)/\Gamma_a\,/[\Delta_a^2 + \tfrac{1}{4}], \text{ and } 1\text{-}n(E_a) = (f'-i\,f'')_{\mathbf{Q}a}\,\rho_{\mathbf{Q}}\,r_0\,\hbar^2c^2/2\pi E_a^2,$$

and the enhancement is given by:

$$|F_{\mathbf{Q},a})|^2 - |F^0_{\mathbf{Q}}|^2 = F^0_{\mathbf{Q}} \sum_a \Re e\mathrm{al}(\alpha_{\mathbf{Q}a})\,(2\Delta_a + \chi'_a)(r_0|\mathbf{M}_{\mathbf{Q}a}|^2/\Gamma_a)/[\Delta_a^2 + \tfrac{1}{4}] + 0^2(r_0|\mathbf{M}_{\mathbf{Q}a}|^2/\Gamma_a)/[\Delta_a^2 + \tfrac{1}{4}]). \qquad (2.4)$$

Thus enhancement and index of refraction oscillations depend on $|\mathbf{M}_{\mathbf{Q}a}|^2$, the classic single electron scattering Thompson radius $r_0 = e^2/mc^2 = 2.82\text{E-}5$Å, the resonance absorption line width, Γ_a=WHH at half amplitude, the separation from resonance $\Delta_a = (\Delta E_L + E_a - h\nu)/\Gamma_a$, where ΔE_L is the Lamb shift, and the electron density $\rho_{\mathbf{Q}} \approx |\sum_l \alpha_{\mathbf{Q}l}\, f_{0l})|/v_c$ where v_c is the volume of the unit cell[2a], and indicate that transitions (1) vary across T_c due to enhanced electron density-structure interactions in all the layers of $YBa_2Cu_3O_{7-\delta}$ (fig. 1-4).

The enhanced XRD [001] reflection (WHH $\leq$ 1eV) versus Cu $L_{3,2}$-E_a (fig. 1a) is used to identify the respective layer contributions by the sign and magnitude of α_{CuO} and α_{CuO_2}(Table **I**) which is in agreement with Cu K-edge XRD-DAFS assignments[2b], but enhanced XAS near the Cu K-E_a[1b] is not resolved at co-incident reflections orientations (fig. 4a, Table **I**) probably because the contribution from α_{CuO} and α_{CuO_2} cancel and/or $|M_{\mathbf{Q},a}|^2$ is not symmetry allowed. Enhanced XAS near the Y K-E_a by co-incident XRD [00L] and [22L] reflections (fig. 4b, Table **I**) indicate that $|M_{\mathbf{Q},a}|^2$ is allowed by symmetry, and there is strong negative enhancement (2.4) at the orientation $\beta = 0^o$ for Y K-edge. The accurate data near the Ba $L_{3,2}$-E_a, at orientation $\beta = 0^o$ obtain $\mu_{0m} = \mu_0 A_m = 2.2$ and 1.4 independent of T, which includes the total material loss, A_m, in agreement with d=6.4μm, and the XAFS, $X_{k,T}$ function[2u] (fig. 2):

$$\ln(A_{E>Ea})_{k,T} = \ln(\mu_{0m,T}(1+X_{k,T})) = \ln(\mu_{0m,T})\{1 + (X_{k,T} - \tfrac{1}{2}\,X_{k,T}^2 + \tfrac{1}{3}\,X_{k,T}^3 ..)/\ln(\mu_{0m,T})\}. \qquad (2.5)$$

At $\beta = 10^o$, the enhancement $e_{T,k} = \ln(A_{T,k}/A_{121K,k})$ is maximum with a deviation versus k (fig. 2c):

$$\Delta e_{k,T} = e_{T,k}/e_{Tc1,k} - 1 = \ln(\mu_{0m,T}/\mu_{0m,Tc1})/\ln(\mu_{0m,Tc1}/\mu_{0m,121K}) *$$

$$\{1 + (X_{k,T} - X_{k,Tc1})(1 + 0^2 ..)/\ln(\mu_{0m,T}/\mu_{0m,Tc1}) + (X_{k,121K} - X_{k,Tc1})(1 + 0^2 ..)/\ln(\mu_{0m,121K}/\mu_{0m,Tc1}) \qquad (2.6)$$

that is independent of $k=(2m_e(E-E_{edge})/\hbar^2)^{1/2}>4/Å$, i.e., the XAFS oscillating terms' contributions cancel out, indicating, within the accuracy of the measurements that there is no structure change across T_{c1} at all orientations, as already determined by Nguyen[1b,d], and the increased absorbance temperature dependence by scattering is the Onsager reciprocal relation to the increased scattering by absorbance, which is determined by the transition moment $|\mathbf{M}_{\mathbf{Q}a}|^2$, when $\boldsymbol{\varepsilon}_0$, $\boldsymbol{\varepsilon}_s$ have non zero components in the Q=[117] and [118] planes (Table **I**).

The temperature dependence of $\mu_{0m,T}$ ($\beta=10^o$) in the interval $121K\geq T \geq 93K$, indicates a mixture of phases is present, say:

$$\mathbf{N}(\text{normal metal})_{T\geq 121K} \Leftrightarrow M(\text{mixed})_{121K\geq T\geq 93K} \Leftrightarrow SC_1(\text{superconducting})_{T\leq 93K}, \qquad (3)$$

where the mixed state absorbance (fig. 2e), and activity are the sum of contributions[2w],

$$<A_{E\geq Eedge,T}> = \mu_{0m,T}(M) = x_{SC1}\ \mu_{0m}(SC_1) + x_N\ \mu_{0m}(N), \quad \text{and} \quad a_M = x_{SC1}\ a_{SC1} + x_N\ a_N,$$

$a = 1$ for pure solids, and x_{SC1} is the mole fraction of the superconducting state in (3). Then:

$$\exp(-\Delta G^{\neq}_{\geq}/k_BT) =(x_{SC1}/x_N)_{121K\geq T\geq Tc1}=[<A_{E\geq Eedge,T}> - <A_{E\geq Eedge,121K}>]/[<A_{E\geq Eedge,Tc1}> - <A_{E\geq Eedge,T}>]$$

obtains the standard state free enthalpy of formation, $\Delta G^{\neq}_{\geq}$ at the two edges to better than 1% reproducibility (fig. 2f), indicating the involvement of the BaO layer chemical activity, by $\Delta H^{\neq}_{\geq}$=-220 meV and $\Delta S^{\neq}_{\geq}$=-2 meV/K and that energy and symmetry are gained in (3). This compares with energy necessary for the reported motion in $YBa_2Cu_3O_{7-x}$, across T_c by anelastic relaxation time measurements, $t = t_{0i}\exp(-W_i/k_BT)$ where (t_{0i}, W_i) = (4E14, 160meV) and (2E-13, 140meV)[2r] which use a fraction of the energy gained for the activation dynamics of atomic oxygen jumps between a, b lattice sites in the CuO_2 layer, at the phase transition that appears to be similar to the correlated and uncorrelated oxygen octahedral rotations in the parent compound, $SrTiO_3$ at the 103 K phase transition[2s], leaving an energy balance, $W_i + \Delta H^{\neq}_{\geq} + 103k_B \approx -50$ meV to form a stable mixed state. Pauling describes the contribution to superconductivity in layer cuprates, by resonance between 2 pure Cu=O covalent bonds forming 90^o to each other, or 4 half covalent and half ionic[1l], which is equivalent to an electron density distribution in the Cu_4O_4 highest occupied states (HOMO) obtained by self consistent field, SCF calculation for the CuO_2 layer in a perfect cuprate lattice using MOTECC-91 codes (fig. 1b)[1f], and similar SCF calculations using METTEC codes for a cluster of 19 unit cells by Sahibudeen[1e] show that the observed PLD with $q_{xy}=2\pi/12(a^2+b^2)^{1/2}$ in the 30 nm film can transfer charge between the CuO_2 and neighboring layers. Additional ordering present below Tc_1 is evident in many measurements

e.g.,[2t, 1b] and a mixture of superconducting phases, say SC_1 and SC_2 is indicated by the rise in A abve T_{c1} (fig. 2e) where the mixture:

$$SC_1(\text{superconducting})_{Tc1\geq T< Tc2} \Leftrightarrow SC_2(\text{superconducting})_{T< Tc2\approx 71.2K},$$

is described by the Gibbs free enthalpy of formation:

$$-\Delta G^{\neq}_{\leq}/k_BT = \ln(x_{SC2}/(1-x_{SC2}))_{Tc1\geq T\geq Tc2} = [A_{E\geq Eedge,T} - A_{E\geq Eedge,Tc1}]/[A_{E\geq Eedge,Tc2} - A_{E\geq Eedge,T}],$$

and indicates that the chemical activity is halved below T_{c1}, $\Delta H^{\neq}_{\leq} = -86$ meV, $\Delta S^{\neq}_{\leq} = -1$ meV/K (fig. 2f), and that the mixture favors ordering.

Thus enhanced XAS/XRD measurements indicate that the Cu:($nd_{5/2,3/2}$), Ba:($nd_{5/2,3/2}$), O:($np_{1/2,3/2}$) and Y:($np_{1/2,3/2}$) electron density contribute significantly to E_HOMO and E_LUMO interactions near T_c, and that there is need for vacuum sites in $YBa_2Cu_3O_{7-\delta}$ (■:insert fig. 1a) for $e_2^{=}$, periodic phonon interactions that lead to BCS type superconductivity[2v]. But, the motion is more complex in $YBa_2Cu_3O_{7-x}$, than in the parent $SrTiO_3$ perovskite due to barriers introduced by an incomplete oxygen octahedral crystal field. The role of $|\mathbf{M}_{\mathbf{Q},a}|^2$ near T_c suggests the possibility to induce the phase transition by photochemical excitation at preferred orientations as has been done in organic superconductors[1m] by cooling the material subject to radiation at preferred orientations to induce transitions between the states:

$$|\text{E\_HOMO}> \Leftrightarrow |\text{E\_LUMO}>, \qquad (4)$$

separated in energy by the shifts observed at say the Cu $L_{3,2}$ E_a, of 0.4 eV (fig, 1a) across T_c.

Conclusion

Chemical activity in $YBa_2Cu_3O_{7-\delta}$, induced near the transition temperature to superconductivity leads to reciprocally enhanced XAS and XRD, at preferred orientations, and identifies the importance of scattering between all the layers at the phase transition, independent of the any prevalent model.

Acknowledgements

The support for work[1] at DOE National Laboratories LBL-ALS, and SLAC-SSRL, IBM Kingston (1991), Trinity and Lucy Cavendish Colleges, Cambridge, and IRC for Superconductivity, Cavendish Laboratory, NSF, and the H. and C. Dreyfus grants at SJSU with valued colleagues (E Clementi, O Stradella, G Corongiu, L Nguyen, CM Burch, ML Chen, MA

Navacerrada, H Sahibudeen, KK Singh, C Chigvinadze, CT Lin and WY Liang) is gratefully acknowledged.

Table I: $YBa_2Cu_3O_{7-\delta}$ scattering parameters near E_a. The laboratory parameters which lead to reciprocally enhanced absorption and scattering are given for orientations in the X-Rays' field, $\beta_{[001]}=\mathbf{k}_0\hat{}\mathbf{c}$, and $\phi_{[001]}=\boldsymbol{\varepsilon}_{[001]}\hat{}\mathbf{a}$ when $(\pi/2-\mathbf{k}_0\hat{}\mathbf{G}_{[HKL]})-\theta_{Bragg}$ is within the XRD line width[a-d]. The crystal parameters (a=3.82, b=3.89, c=11.68 Å in D_{2h}^1 Space Group) and f^0_1 Cromer Mann Atomic Scattering Tables[2g], obtain $\theta(E_a)$ and F^0_Q when the Bragg condition is satisfied for an XRD [HKL] reflection plane.

Absorber a parameters:	O-K	Cu-L2,3	Ba-L3	Ba-L2	Cu-K	Cu-K	Cu-K	Y- K	Y- K	Y- K	Y- K	Y- K	Y- K
H	0	0	1	1	0	1	1	0	0	0	2	0	0
K	0	0	1	1	0	0	1	0	0	0	2	0	0
L	1	1	7	8	17	16	9	29	32	28	27	23	33
$Q_{[HKL]}$ (1/Å)	0.538	0.538	4.416	4.883	9.145	8.763	5.363	15.600	17.214	15.062	15.239	12.372	17.751
D^1_{4h}: F^0_Q	-5.9	-5.9	-45.4	-34.8	-29.0	-28.2	-33.6	30.0	39.2	33.7	24.6	2.2	18.0
measured E_a (eV)	540	924	5255	5627	9023	8990	8990	17047	17047	17047	17047	17047	17515
$\theta_{Bragg,Ea}$ (°)	79.37	35.06	56.01	58.89	89.43	74.09	36.06	64.54	85.06	60.66	61.89	45.73	89.51
Element Enhance													
$\Sigma\alpha_{a\,1}\,F^0_Q/\lvert F^0_Q\rvert^2=$	-0.17	-0.17	0.01	0.06	-0.03	-0.04	-0.03	0.03	0.03	0.03	-0.04	-0.45	-0.06
$\Sigma\alpha_{a\,2}\,F^0_Q/\lvert F^0_Q\rvert^2=$	-0.18	0.21			0.03	0.07	-0.03						
$\Sigma\alpha_{a3}\,F^0_Q/\lvert F^0_Q\rvert^2=$	0.49												
measured:													
$\beta_{[001]}$ (°)	6.61	60.5	10	10	10	15	45	25	5	30	20	45	0
$\phi_{[001]}$ (°)	0.0	0.0	7.5	7.5	7.5	7.5	7.5	7.5	7.5	7.5	7.5	7.5	7.5
$E_{Bragg}(\beta)$ (eV)	534	1078	5279	5627	9162	9139	8841	16983	17048	17160	16969	17263	17514
$\theta_{Bragg,Ea}(\beta,\phi)$	83.39	29.50	55.62	58.89	80	71	37	65	85	60	62	45	90
$\varepsilon_{[001]}\hat{}G_{[110]}$ -45(°)	0.4	24.6	8.2	8.2	8.2	9.0	19.5	11.5	7.7	13.2	10.1	19.5	7.5
% $\Delta\theta_{Bragg}/\theta$	5%	-17%	-1%	0%	-11%	-4%	2%	1%	0%	-1%	1%	-2%	1%
% $\Delta E_{Bragg}/E$	-1.1%	15.4%	0.5%	0.0%	1.5%	1.6%	-1.7%	-0.4%	0.0%	0.7%	-0.5%	1.3%	0.0%

a. Enhanced XRD $I_{[001]}$ reflection, near O K, and Cu $L_{2,3}$-E_a, proportional to $\alpha_{a,\mathbf{Q}}F^0_Q/|F^0_Q|^2$ is observed when deviations $\Delta\theta/\theta$, and $\Delta E/E$ are within the scattering line widths in (2.3) of the order of 10% to 20% (fig. 1a, 3a), and fluorescence is negligible at 2θ.

b. Near the Ba $L_{3,2}$-E_a the scattering enhancement of absorbance appears as an increase in A, and $n(E_a)$ critical oscillations[1b].

c. At the Cu K-edge $(\alpha_{Cu(1)} + 2\alpha_{Cu(2)})F^0_Q$ mostly cancel.

d. Near the Y K-E_a the [00 33] and [00 23] at the respective orientations $\beta_{[001]}=0$, 45° introduce shifts and $n(E_a)$ critical oscillations.

List of Figures

Figure 1: $YBa_2Cu_3O_{7-\delta}$ 30 nm film on $SrTiO_3$[1i]: **(a)** Temperature cycle of XRD $I_{[001]}$ reflection enhanced near the Cu $L_{3,2}$-E_a ($\Delta Q_{[001]} \approx 0.01$ to 0.03 $Å^{-1}$)[1e], over 24 h in the JB Kortright chamber at DOE-LBL-ALS[2j], indicates edge shifts of ~0.4 eV and intensity doubling below T_c where a c-axis decrease below T_c of 0.1%[2l] would propagate to a further decrease in $\Delta\theta/\theta_{Bragg}$ (Table **I**) and therefore $I_{[001]}$. Cartoon insert describes the layer stacking in the ideal D_{4h}^1 Space Group[2 i,k,l] with unit cell sites indicated by: open square □:front, closed square ▪:back, and presumed element occupation by different shades, ▬:Ba, ▬:Cu, ▬:Y, ▬:O, and ▬:vacuum sites which are important for synchronized and unsynchronized motion between occupied sites, and the layers orientation relative to the incident X-Rays' $\beta_{[001]}$ = **c**^I_0. **(b)** Cu_4O_4 electron density for the molecular basis set for E_HOMO and E_LUMO obtained by self consistent crystal field calculations of layer cuprates using MOTECC-91 codes[1f], describe the σ-bonded O:O chains responsible for transport in different representations which also include p_z molecular orbital symmetry within 10 eV of Rydberg states.

Figure 2: Single crystal CT-$YBa_2Cu_3O_{7-\delta}$ Ba $L_{3,2}$-edge absorption, A enhanced by reciprocal scattering near T_c at certain orientations[1b]: **(a)** Near edge absorbance, A(T, $\beta_{[001]}$) versus E_a, at different T near T_c when $\beta_{[001]}=10\pm1^o$: ▬: 121 to 100K, ▬: 99 to 95 K, ▬ 93 to 92K, ▬ 88 to 70K, and ▬ 69 to 56K, and when $\beta_{[001]}=0$, and 5 ± 1^o ▬, and ▬ respectively between T=121 to 56K A appear unchanged. **(b)** $Ln(A_{E>Ea})=ln(\mu_0(1+X))$ versus $E>E_a$. **(c)** Enhancement deviation (2.6) at $\beta = 10^o$, $\Delta e_{k,T} = ln(A_T/A_{93K})/ln(A_{93K}/A_{121K})-1$ versus $|\mathbf{k}|=\sqrt{(2m_e(E-E_{edge})/\hbar^2)}$. **(d)** Cartoons of layer orientation relative to incident, transmitted and scattered X-Rays, $I_{0j}=T_j$, T_{0j+1}, S_j. respectively. **(e)** Absorbance averaged over all k (230 data points at each T), $<A>_k$ versus 1/T near T_c when $\beta_{[001]}=10\pm1^o$. **(f)** Ratio, $ln(x_{SC}/(1- x_{SC}))$ versus 1/T used to obtain the standard free enthalpy for the formation of mixed states, by linear fits. For $T\geq T_{c1}=92K$: $E>E_{L3}$:♦, $E>E_{L2}$:■, and for $T_{c1}\geq T\leq T_{c2}\approx 71K$: $E>E_{L3}$:+, $E>E_{L2}$:**x**. For $T\geq$ 92K the fit accuracy, R2=0.99 is better than for $92\geq T\geq$ 71K, of R2=0.93.

Figure 3: $YBa_2Cu_3O_{7-\delta}$ 30 nm film on $SrTiO_3$ $I_{[001]}$ for reversible temperature cycle near O K-E_a, $\Delta Q_{[001]} \approx$ -0.04 to 0.06 $Å^{-1}$[1i]. Sites' are identified by the phase $\alpha_{\mathbf{Q},a}$ sign for the enhancement (Table **I**) in agreement with the literature[2m]. Changes in $I_{[001]}$ below T_c suggest state occupation changes below T_c.

Figure 4: Single crystal CT-$YBa_2Cu_3O_{7-\delta}$ A[1b]. **(a)** Cu K-E_a and. **(b)** Y K- K-E_a. Critical index of refraction n(E_a), oscillations, and negative/positive enhancement indicates the element involvement near T_c (Table **I).**

. References

1. **(a)** JV Acrivos, ML Chen and CM Burch, *Superlattices and Microsturctures*, **18**, 197 (1995); **(b)** JV Acrivos, L Nguyen, T Norman, CT Lin, WY Liang, JM Honig and J Somasundaram, *Microchemical Journal*, **71**, 117-131 (2002); **(c)** JV Acrivos, L Chen, CM Burch, P Metcalf, JM Honig, RS Liu and KK Singh, *Phys. Rev. B* **50**, 13710 (1994); **(d)** L Nguyen, MS Thesis, SJSU (2000) **(e)** HS Sahibudeen, MA Navacerrada and JV Acrivos, *NanoTech 2005* **2**, 573 (2005); MA Navacerrada and JV Acrivos, *NanoTech 2003,* **1**, 751 (2003); **(f)** J.V. Acrivos and O Stradella, *International Journal of Quantum Chemistry*, **46**, 55(1993); **(g)** JV Acrivos, ML Chen, C Jiang, H. Nguyen, P Metcalf and J M Honig, *J. Solid State Chemistry,* **111**, 343 (1994); **(h)** JV Acrivos *et al., Solid State Sciences*, **2**, 807 (2000); **(i)** J.V. Acrivos L. Nguyen, H.S. Sahibudeen, P. Nachimuthu and M.A. Navacerrada, http://arxiv.org/cond-mat/0504369; **(j)** JV Acrivos, MP Klein, A Thompson et al., *Rev. Sci. Instrum.* **53**, 575 (1982); (**k**) CT Lin and WY Liang, *Physica* **C195**, 291 (1992); *ibid,* **C225**, 271 (1994); (**l**) L Pauling, *Phys. Rev. Lett.,* **59**, 225 (1988);(**m**) JV Acrivos, HP Hughes and SSP Parkin, *J. Chem. Phys.* **86,** 1780 (1987); (**n**) JV. Acrivos, *Mol. Cryst. Liq. Cryst*., **284**, 411 (1996)

2. **(a)** RW James, *The Optical Principles of The Diffraction of X-rays*, Oxbow Press, (1946, 1982); **(b)** LB Sorensen et al., "*Resonant Anomalous X-Ray Scattering", Elsevier Science* G Materlik et al., ed , p389 (1994); **(c)** AW Overhauser et al., *Phys. Rev. B* **61**, 1885 (1988); **(d)** PG de Gennes, *Rev. Mod. Phys.* **36**, 225 (1964) **(e)** JV Acrivos, *Physics and Chemistry of Electrons and Ions in Condensed Matter,* NATO ASI Series C**130,** 479 (1983), JV Acrivos, NF Mott and AD Yoffe, ed.; **(f)** LK Templeton and DH Templeton, *Acta Cryst. A* **47**, 414 (1991); **(g)** http://www.cxro.lbl.gov; **(h)** JV Acrivos et al., http://arxiv.org/cond-mat/0504369; **(i)** EE Koch, Handbook on Synchrotron Radiation, North Holland Pub. Co, The Netherlands (1983) Ch. 7 and 9; **(j)** JB Kortright, SSP Parkin, et al., *J. Magn. Magn. Materials*, **207**, 7-44 (1999); *ibid*, **62**, 12216 (2000); **(k)** JM Tarascon et al., *Phys. Rev B* **37**, 9382 (1988)*;ibid,* **38**, 8885 (1989), **(l)** RM Hazen et al., "*Physical Properties of High Temperature Superconductors, II*", p.121, DM Ginsberg, ed. *World Scientific* (1990); **(m)** N Nücker et al., *Phys. Rev. **B*** **51**, 8529 (1995); **(n)** JG Chigvinadze, JV Acrivos, et al., , *Physics Letters* **A 373,** 874 (2009); **(o)** VM Pan et al.,: *Low Temperature Physics*, .**27**, 732, (2001); **(p)** G Chigvinadze, G. Mamniashvilli, JV Acrivos, http://arxiv.org/cond-mat/0508052**; (q)** V Ginzburg, *Soviet Physics Uspekhi,* **5**, 649 (1963); **(r)** G Cannelli et al., *Physica C*1**53-155,** 298 (1988); **(s)** R Wang, Y Zhu, SM Shapiro, *Phys Rev B* **61**,8814 (2000); **(t)** HA Blackstead and JD Dow, *Physica C* **235-240***, 1363* (1994), *JETP Lett.*, **59**, 283 (1994); **(u)** BK Teo, *"EXAFS"*, Springer-Verlag, Berlin (1986); **(v)** J Bardeen et al., *Phys. Rev. B **106, 162, ibid,*** **108**, 1175 (1957); (**w**) KS Pitzer, "Thermodynamics", 3rd ed McGraw-Hill (1995)

Figure 1(a)

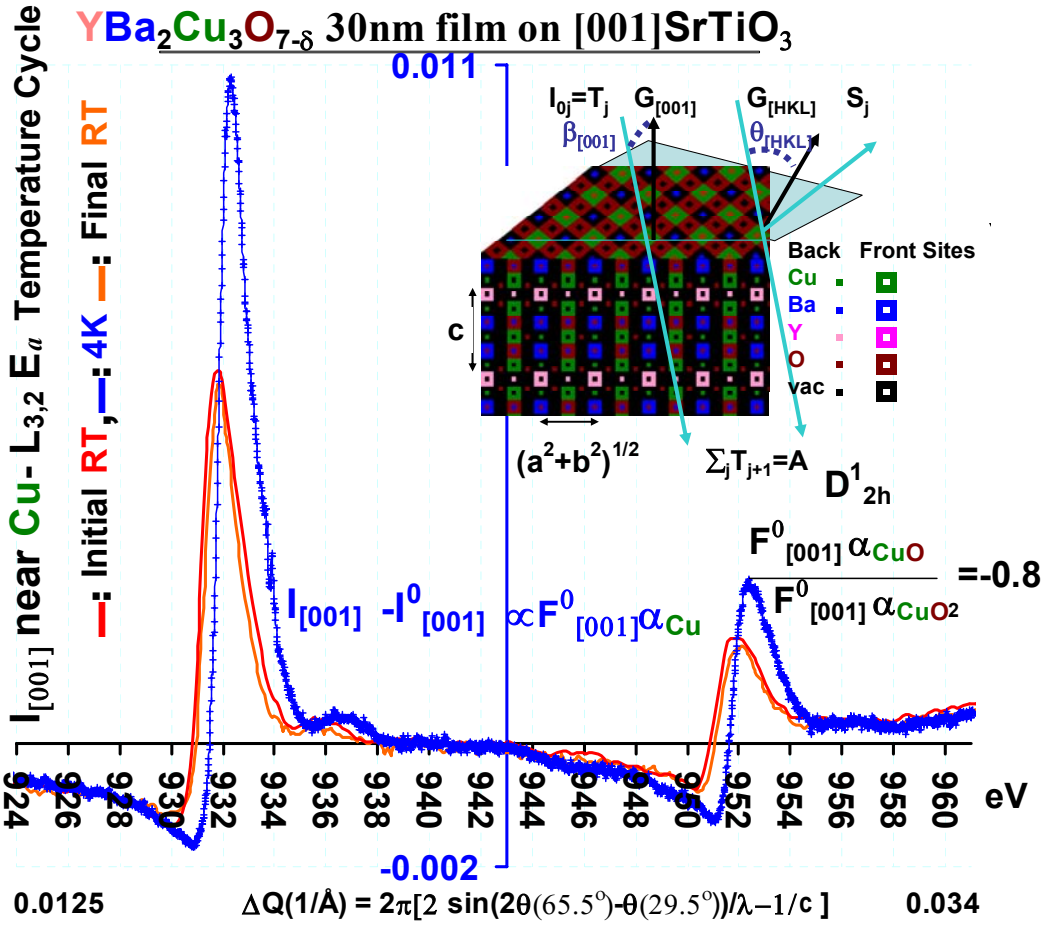

Figure1(b)

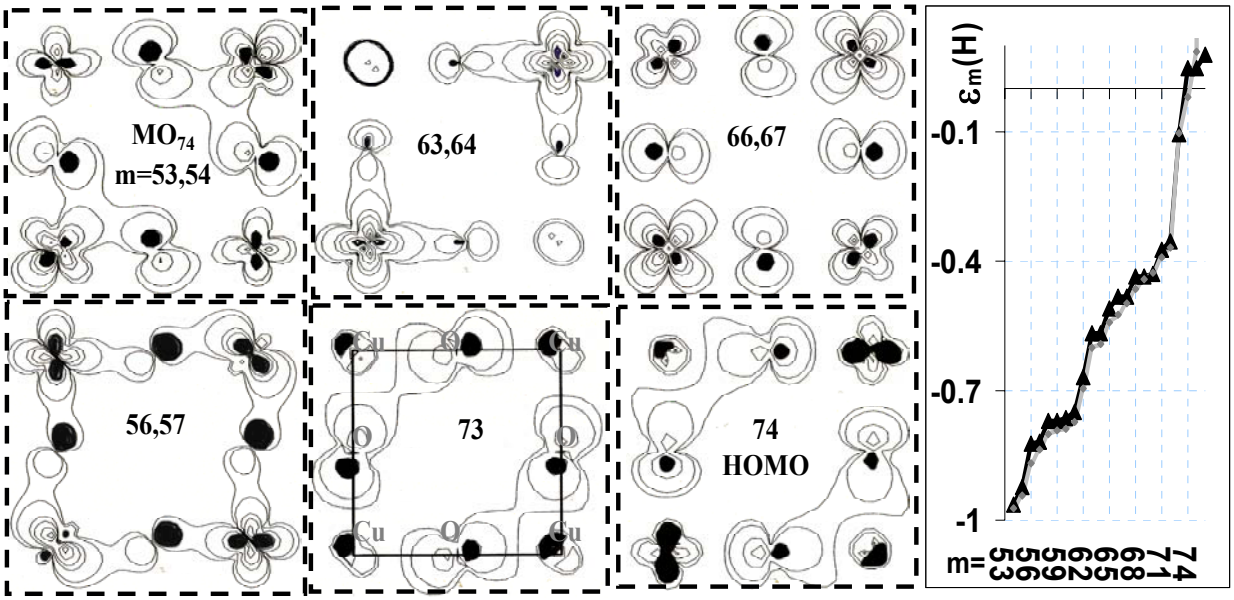

Figure 2 :

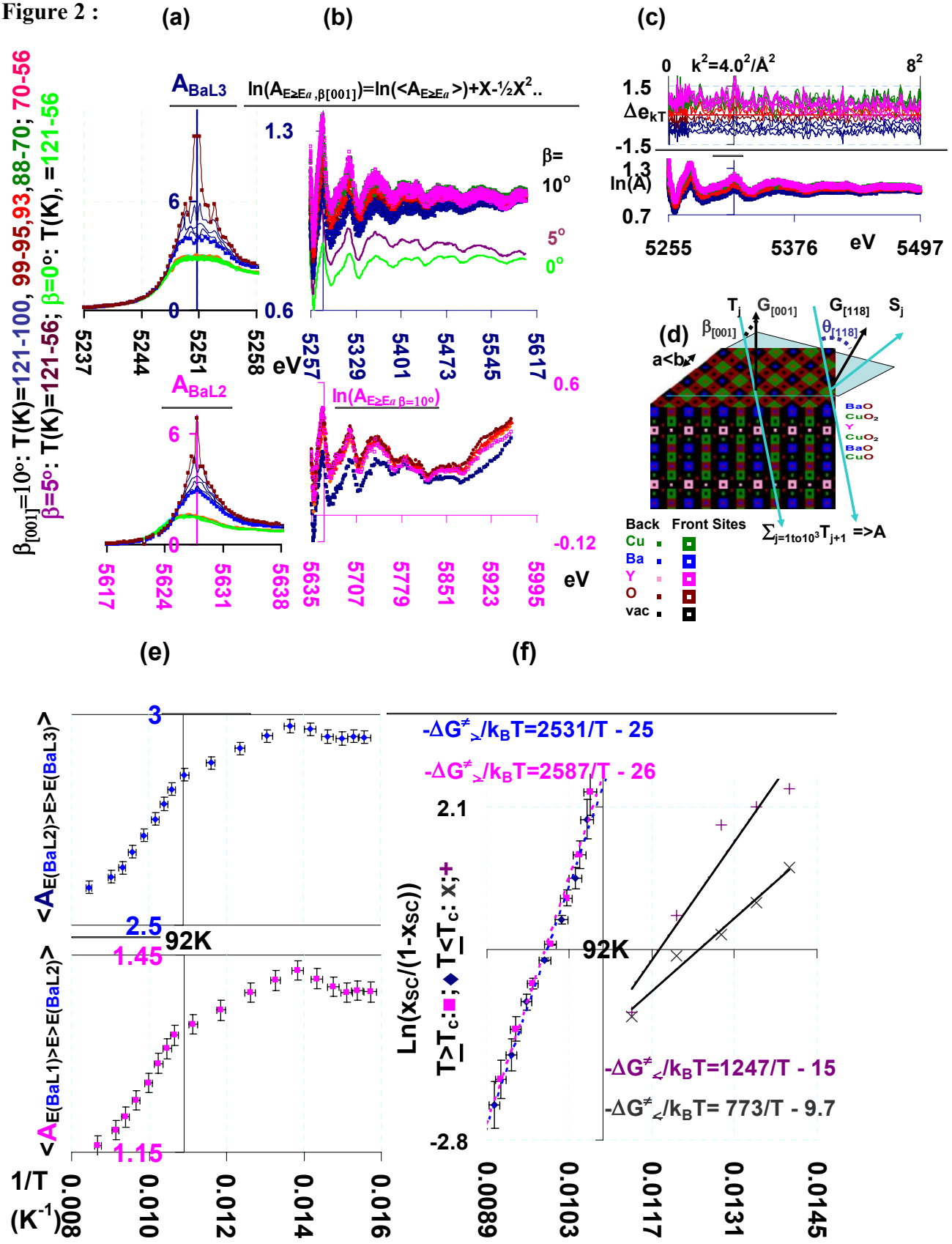
(a)
(b)
(c)
(d)
(e)
(f)
$\beta_{[001]}$=10°: T(K)=121-100, 99-95,93,88-70; 70-56
β=5°: T(K)=121-56; β=0°: T(K), =121-56
A_{BaL3}
$\ln(A_{E\geq E\alpha,\beta[001]})=\ln(<A_{E\geq E\alpha}>)+X-½X^2..$
β=
10°
5°
0°
eV
A_{BaL2}
$\ln(A_{E\geq E\alpha\ \beta=10°})$
$k^2=4.0^2/Å^2$
Δe_{kT}
ln(Ā)
5255
5376
5497
T_j
$G_{[001]}$
$G_{[118]}$
S_j
$\beta_{[001]}$
$\theta_{[118]}$
a<b
BaO
CuO_2
Y
CuO_2
BaO
CuO
Back
Front Sites
Cu
Ba
Y
O
vac
$\sum_{j=1to10^3} T_{j+1}$ =>A
$<A_{E(BaL2)>E>E(BaL3)}>$
$<A_{E(BaL1)>E>E(BaL2)}>$
92K
1/T
(K^{-1})
$-\Delta G^{\neq}_{\geq}/k_BT=2531/T - 25$
$-\Delta G^{\neq}_{\geq}/k_BT=2587/T - 26$
$-\Delta G^{\neq}_{\leq}/k_BT=1247/T - 15$
$-\Delta G^{\neq}_{\leq}/k_BT= 773/T - 9.7$
$Ln(x_{SC}/(1-x_{SC}))$
$T\geq T_c$:■; ◆ $T<T_c$: x; +

Figure 3

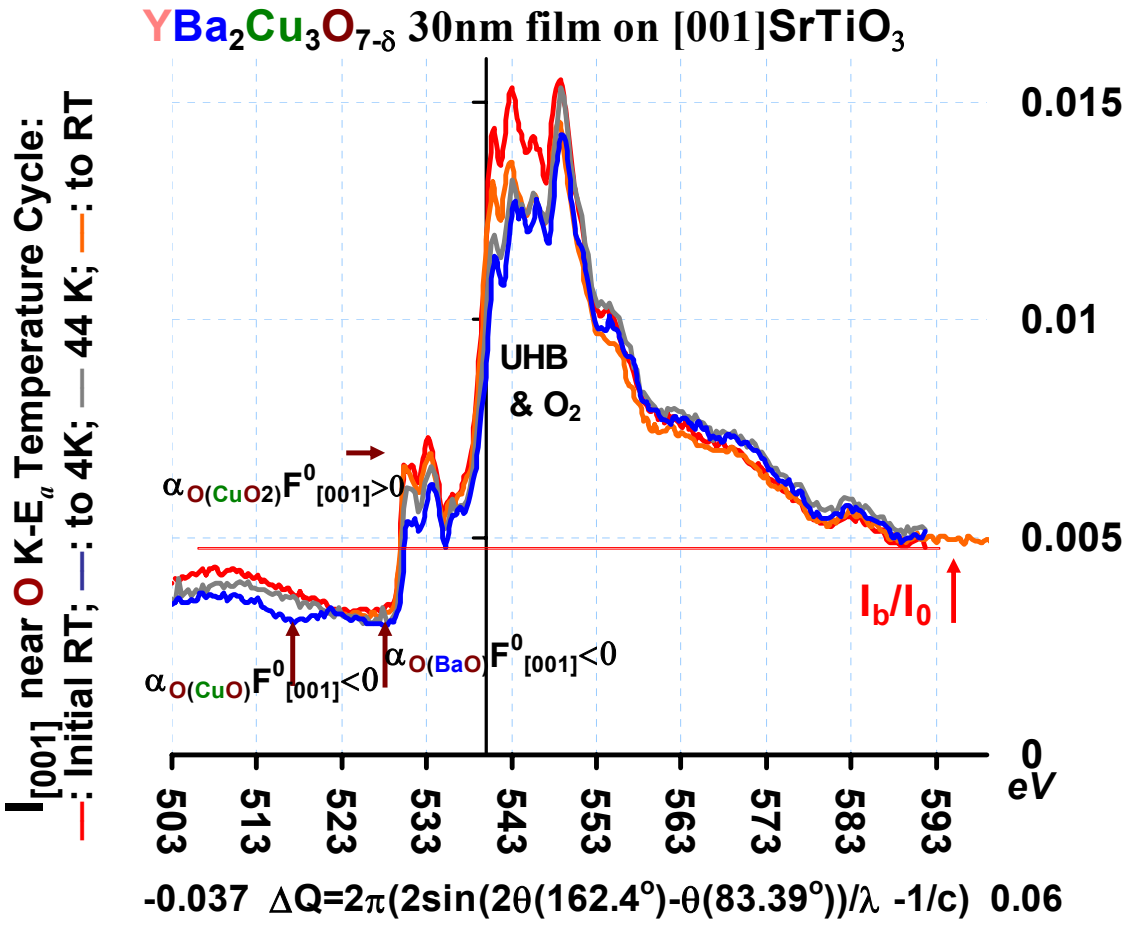
YBa2Cu3O7-δ 30nm film on [001]SrTiO3
I[001] near O K-Eα Temperature Cycle:
—: Initial RT; —: to 4K; —: 44 K; —: to RT
0.015
0.01
0.005
0
UHB
& O2
αO(CuO2)F0[001]>0
αO(CuO)F0[001]<0
αO(BaO)F0[001]<0
Ib/I0
eV
503
513
523
533
543
553
563
573
583
593
-0.037 ΔQ=2π(2sin(2θ(162.4°)-θ(83.39°))/λ -1/c) 0.06

Figure 4:

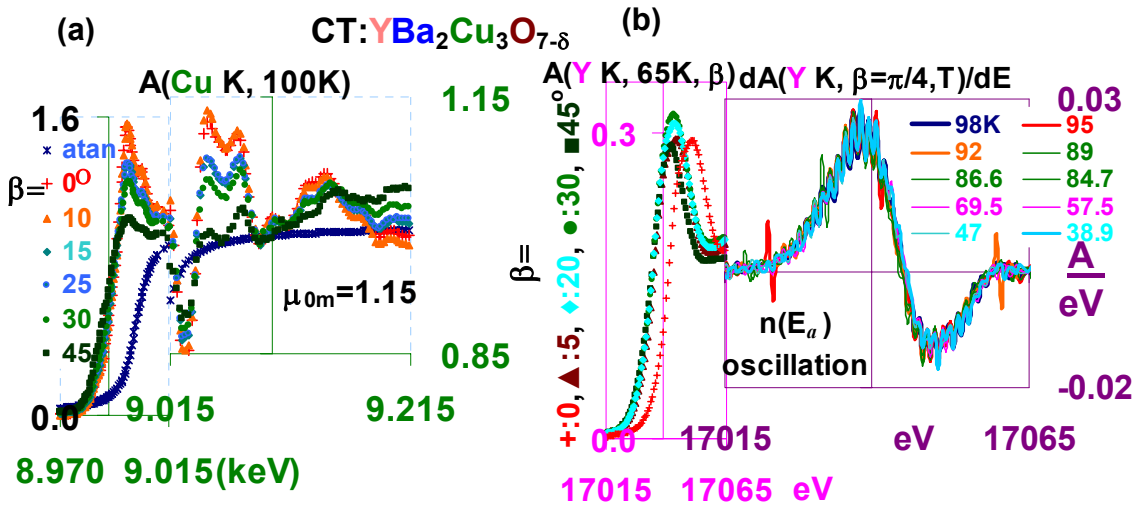
(a)
CT:YBa2Cu3O7-δ
A(Cu K, 100K)
1.6
1.15
0.85
0.0
9.015
9.215
8.970 9.015(keV)
atan
β= 0°
10
15
25
30
45
μ0m=1.15
(b)
A(Y K, 65K, β)
dA(Y K, β=π/4,T)/dE
β= +:0, ▲:5, ♦:20, ●:30, ■45°
0.3
0.0
17015
17065 eV
98K
92
86.6
69.5
47
95
89
84.7
57.5
38.9
n(Ea)
oscillation
0.03
-0.02
A
eV
17015 17065 eV